Mathematical Biosciences and Engineering

http://www.aimspress.com/journal/MBE

MBE, 17(2): 1074–1089.
DOI: 10.3934/mbe.2020057
Received: 29 July 2019
Accepted: 07 November 2019
Published: 14 November 2019

Research article

Optimizing vaccination strategies in an age structured SIR model

Rinaldo M. Colombo[1] **and Mauro Garavello**[2,*]

[1] INdAM Unit, University of Brescia, via Branze, 38, 25123 Brescia, Italy

[2] Department of Mathematics and its Applications, University of Milano – Bicocca, via R. Cozzi, 55, 20126 Milano, Italy

* **Correspondence:** Email: mauro.garavello@unimib.it.

Abstract: We present a modeling framework based on a structured SIR model where different vaccination strategies can be tested and compared. Vaccinations can be dosed at prescribed ages or at prescribed times to prescribed portions of the susceptible population. Different choices of these prescriptions lead to entirely different evolutions of the disease. Once suitable *"costs"* are introduced, it is natural to seek, correspondingly, the *"best"* vaccination strategies. Rigorous results ensure the Lipschitz continuous dependence of various reasonable costs on the control parameters, thus ensuring the existence of optimal controls and suggesting their search, for instance, by means of the steepest descent method.

Keywords: optimal control; deterministic epidemics; Conservation Laws; renewal equations; hyperbolic SIR model

1. Introduction

Within the framework of a nonlocal SIR model, we introduce different vaccination policies and then seek the most effective one. Vaccines are dosed at prescribed ages or at prescribed times to prescribed portions of the susceptible population. The careful choice of the ages, times and individuals to be treated may significantly influence the efficiency of a vaccination campaign. It is thus natural to tackle the resulting optimal control problem, seeking what is in some sense the best vaccination policy.

We denote by $S = S(t, a)$ the density of individuals at time t of age a susceptible to the disease. As usual, $I = I(t, a)$ is the density of infected individuals at time t and of age a. The density of individuals that can not be infected by the disease is $R = R(t, a)$, comprising individuals that recovered as well as those that are, whatever the reason, immune. As a reference to the basic properties of SIR models, originated in [1], see [2, Chapter 6], [3, Chapter 19] or [4, § 1.5.1].

A possible description of the evolution of S is provided by the renewal equation [4, Chapter 3] with

nonlocal source term

$$\partial_t S + \partial_a S = -\left(d_S(t,a) + \int_0^{+\infty} \lambda(a,a')\, I(t,a')\, \mathrm{d}a'\right) S \tag{1.1}$$

where $d_S = d_S(t,a) \geq 0$ is the susceptibles' death rate and $\lambda(a,a') \geq 0$ quantifies the susceptible individuals of age a that are infected by individuals of age a'. The nonlocal quantity on the right hand side of (1.1), namely $\int_0^{+\infty} \lambda(a,a')\, I(t,a')\, \mathrm{d}a'\, S(t,a)$, represents the total number of susceptible individuals of age a that become infected at time t per unit time.

The evolution of the infected portion I of the population is governed by

$$\partial_t I + \partial_a I = -\left(d_I(t,a) + r_I(t,a)\right) I + \int_0^{+\infty} \lambda(a,a')\, I(t,a')\, \mathrm{d}a'\, S, \tag{1.2}$$

where $d_I = d_I(t,a) \geq 0$ is the death rate of the I portion of the population and $r_I = r_I(t,a) \geq 0$ represents the fraction of infected individuals of age a that recovers at time t per unit time. Finally, the evolution of the portion R of the population that recovers or is unaffected from the disease is

$$\partial_t R + \partial_a R = r_I(t,a)\, I - d_R(t,a)\, R\,, \tag{1.3}$$

where $d_R = d_R(t,a) \geq 0$ is the death rate of the R population. We assume here that members of the R population are not dosed with vaccine and that individuals may enter the R population at birth. In the present setting, dealing with choices different from these latter ones only requires very minor changes and keeps falling in the present general analytic framework.

In a first policy, vaccinations are dosed at any time t at a time dependent portion $\eta_j(t)$ of the S population of the prescribed age $\bar{a}_j$, with $0 < \bar{a}_1 < \cdots < \bar{a}_N$. In this way, the fraction $\eta_j(t)$ of susceptible population $S(t,\bar{a}_j)$ becomes immune. In other words, we use as control the fractions $\eta_j \colon \mathbb{I} \to [0,1]$ (for $j \in \{1,\cdots,N\}$ and $\mathbb{I}$ being the, possibly unbounded, time interval under consideration). We thus have to supplement the evolution (1.1)–(1.2)–(1.3) with the vaccination conditions

$$\begin{array}{rcll} S(t,\bar{a}_j+) & = & \left(1-\eta_j(t)\right) S(t,\bar{a}_j-) & [\forall t,\, S(t,\bar{a}_j) \text{ decreases due to vaccination}] \\ I(t,\bar{a}_j+) & = & I(t,\bar{a}_j-) & [\text{the infected population is unaltered}] \\ R(t,\bar{a}_j+) & = & R(t,\bar{a}_j-) + \eta_j(t)\, S(t,\bar{a}_j-) & [\text{vaccinated individuals are immunized}] \end{array} \tag{1.4}$$

for a.e. $t > 0$ and for $j \in \{1,\cdots,N\}$. A reasonable constraint on the vaccination policy η in (1.4) is that its total cost $\mathcal{N}(\eta)$ on the considered time interval $\mathbb{I}$ does not exceed a prescribed maximal cost M. Measuring the total cost by the number $\mathcal{N}$ of dosed individuals, we have

$$\mathcal{N}(\eta) \leq M \quad \text{where} \quad \mathcal{N}(\eta) = \sum_{i=1}^{N} \int_{\mathbb{I}} \eta_i(t)\, S(t,\bar{a}_i-)\, \mathrm{d}t\ . \tag{1.5}$$

Alternatively, we also consider vaccination campaigns immunizing an age dependent portion of the whole population at given times $\bar{t}_1, \ldots, \bar{t}_N$. This amounts to substitute (1.4) with

$$\begin{array}{rcll} S(\bar{t}_k+,a) & = & \left(1-\nu_k(a)\right) S(\bar{t}_k-,a) & [\forall a,\, S(\bar{t}_k,a) \text{ decreases due to vaccination}] \\ I(\bar{t}_k+,a) & = & I(\bar{t}_k-,a) & [\text{the infected population is unaltered}] \\ R(\bar{t}_k+,a) & = & R(\bar{t}_k-,a) + \nu_k(a)\, S(\bar{t}_k-,a) & [\text{vaccinated individuals are immunized}] \end{array} \tag{1.6}$$

where $\nu_k(a)$ is the percentage of susceptible individuals of age a that are dosed with the vaccine at time $\bar{t}_k$, for $k = 1, \dots, N$. Now, a reasonable constraint due to the campaign cost is given by a bound on the number $\mathcal{N}$ of dosed individuals

$$\mathcal{N}(\nu) \le M \quad \text{where} \quad \mathcal{N}(\nu) = \sum_{i=1}^{N} \int_{\mathbb{R}^+} \nu_i(a)\, S(\bar{t}_i-, a)\, \mathrm{d}a \ . \tag{1.7}$$

For simplicity, in both cases above, we assume that η_j, respectively ν_i, represents the percentages of individuals that are *successfully* vaccinated.

In both cases, our aim is to seek the vaccination campaign that minimizes the total number of infected individuals of all ages over the time interval $\mathbb{I}$, that is

$$\mathcal{J} = \int_{\mathbb{I}} \int_{\mathbb{R}^+} \varphi(a)\, I(t, a)\, \mathrm{d}a\, \mathrm{d}t \tag{1.8}$$

the function φ being a suitable positive age dependent weight. Here, $\mathcal{J}$ is a function of η in case (1.4) and of ν in case (1.6). In general, in the two cases (1.4) and (1.6), reasonable costs are thus

$$\mathcal{J}(\eta) + \mathcal{N}(\eta) = \int_{\mathbb{I}} \int_{\mathbb{R}^+} \varphi(a)\, I(t, a)\, \mathrm{d}a\ \mathrm{d}t + \sum_{j=1}^{N} \int_{\mathbb{I}} \eta_j(t)\, S(t, \bar{a}_j-)\, \mathrm{d}t \tag{1.9}$$

$$\mathcal{J}(\nu) + \mathcal{N}(\nu) = \int_{\mathbb{I}} \int_{\mathbb{R}^+} \varphi(a)\, I(t, a)\, \mathrm{d}a\ \mathrm{d}t + \sum_{i=1}^{N} \int_{\mathbb{R}^+} \nu_i(a)\, S(\bar{t}_i-, a)\, \mathrm{d}a \ . \tag{1.10}$$

Clearly, in general, suitable weights can be used to modify the relative relevance of the two costs $\mathcal{N}$ and $\mathcal{J}$ in the sums above.

The current literature offers a variety of alternative approaches to similar modeling situations. In the context of models based on ordinary differential equations, that is, without an age structure in the population, this problem has been considered, for instance, already in [5–7]. In the recent [8], the vaccination control enters an equation of the type (1.1) through a term $-u\,S$ in the source on the right hand side of (1.1), implicitly suggesting that vaccination takes place uniformly at all ages. For a recent related investigation focused on cholera, see [9].

The next section summarizes the key analytic properties of the present SIR model, providing the necessary basis to tackle optimal control problems. Section 3 shows the qualitative properties of various vaccination strategies through numerical integrations. Section 4 presents numerical optimizations through the descent method. The paper ends with Section 5.

2. Well posedness and stability properties of the models

Denote by $\mathbb{I}$ either the time interval $[0, T]$, for a positive T, or $[0, +\infty[$. Fix throughout a positive integer N representing the number of vaccination sessions.

Both models introduced above lead to the initial – boundary value problem

$$\begin{cases} \partial_t S + \partial_a S = -\left(d_S(t, a) + \int_0^{+\infty} \lambda(a, a')\ I(t, a')\, \mathrm{d}a'\right) S \\ \partial_t I + \partial_a I = -\left(d_I(t, a) + r_I(t, a)\right) I + \int_0^{+\infty} \lambda(a, a')\, I(t, a')\, \mathrm{d}a'\ S \\ \partial_t R + \partial_a R = r_I(t, a) I - d_R(t, a)\, R \end{cases} \tag{2.1}$$

with initial datum and boundary inflow

$$\begin{cases} S(0,a) = S_o(a), & I(0,a) = I_o(a), & R(0,a) = R_o(a), & a \in \mathbb{R}^+; \\ S(t,0) = S_b(t), & I(t,0) = I_b(t), & R(t,0) = R_b(t), & t \in \mathbb{I}\,. \end{cases} \tag{2.2}$$

The usual case of the birth terms in the boundary data being assigned through suitable integrals of the populations in reproductive age can be recovered by mainly technical adjustments.

We assume below that the following assumptions are satisfied:

(λ) $\lambda \in \mathbf{C}^0(\mathbb{R}^+ \times \mathbb{R}^+; \mathbb{R})$ is bounded, with total variation in the first argument uniformly bounded with respect to the second (i.e., $\sup_{a' \in \mathbb{R}^+} \mathrm{TV}\,(\lambda(\cdot, a'); \mathbb{R}^+) < +\infty$) and Lipschitz continuous in the first argument uniformly with respect to the second (i.e., there exists a $C > 0$ such that for all $a, a_1, a_2 \in \mathbb{R}^+$, $|\lambda(a_1, a') - \lambda(a_2, a')| \le C\,|a_1 - a_2|$).

(d-r) The maps $d_S, d_I, d_R, r_I \colon \mathbb{I} \times \mathbb{R}^+ \to \mathbb{R}$ are bounded Caratheodory functions, with $\mathbf{L}^1$ norm and total variation in a uniformly bounded in t (i.e., for $\varphi = d_S, d_I, d_R, r_I$, $\sup_{t \in \mathbb{I}} \|\varphi(t)\|_{\mathbf{L}^1(\mathbb{R}^+;\mathbb{R})} < +\infty$ and $\sup_{t \in \mathbb{I}} \mathrm{TV}\,(\varphi(t, \cdot); \mathbb{R}^+) < +\infty$) and Lipschitz continuous in a uniformly in t (i.e., there exists a $C > 0$ such that for all $t \in \mathbb{I}$ and $a_1, a_2 \in \mathbb{R}^+$, $|\varphi(t, a_2) - \varphi(t, a_1)| \le C\,|a_2 - a_1|$).

(IB) The initial datum and the boundary inflow in (2.2) satisfy $S_o, I_o, R_o \in (\mathbf{L}^1 \cap \mathbf{BV})(\mathbb{R}^+; \mathbb{R}^+)$ and $S_b, I_b, R_b \in (\mathbf{L}^1 \cap \mathbf{BV})(\mathbb{I}; \mathbb{R}^+)$.

For the definition of Caratheodory function, of total variation and of the various functional spaces, we refer for instance to [10]. For all other analytic details specific to the present construction, see [11].

First, we provide the basic well posedness and stability result for the model (2.1)–(2.2) in the case of the vaccination policy (1.4), namely

$$\begin{cases} S(t, \bar a_j+) = \big(1 - \eta_j(t)\big)\, S(t, \bar a_j-) \\ I(t, \bar a_j+) = I(t, \bar a_j-) \\ R(t, \bar a_j+) = R(t, \bar a_j-) + \eta_j(t)\, S(t, \bar a_j-) \end{cases} \qquad j = 1, \dots, N\,. \tag{2.3}$$

Theorem 2.1 ([11]). *Under hypotheses (λ) and **(d-r)**, for any initial and boundary data satisfying **(IB)**, for any choice of the positive vaccination ages $\bar a_1, \dots, \bar a_N \in \mathbb{R}^+ \setminus \{0\}$ and of the control function $\eta \in \mathbf{BV}(\mathbb{I}; [0,1]^N)$, problem* (2.1)–(2.2)–(2.3) *admits a unique solution defined on the whole interval $\mathbb{I}$, depending Lipschitz continuously on the initial datum, through the $\mathbf{L}^1$ norm, and on η, through the $\mathbf{L}^\infty$ norm.*

An entirely similar result holds for the vaccination policy (1.6), which we rewrite here as

$$\begin{cases} S(\bar t_i+, a) &=& \big(1 - \nu_i(a)\big)\, S(\bar t_i-, a) \\ I(\bar t_i+, a) &=& I(\bar t_i-, a) \\ R(\bar t_i+, a) &=& R(\bar t_i-, a) + \nu_i(a)\, S(\bar t_i-, a)\,. \end{cases} \qquad i = 1, \dots, N\,. \tag{2.4}$$

Theorem 2.2 ([11]). *Under hypotheses (λ) and **(d-r)**, for any initial and boundary data satisfying **(IB)**, for any choice of the positive vaccination times $\bar t_1, \dots, \bar t_N \in \mathbb{I} \setminus \{0\}$ and of the control function $\nu \in \mathbf{BV}(\mathbb{R}^+; [0,1]^N)$, problem* (2.1)–(2.2)–(2.4) *admits a unique solution defined on the whole interval $\mathbb{I}$, depending Lipschitz continuously on the initial datum, through the $\mathbf{L}^1$ norm, and on ν, through the $\mathbf{L}^\infty$ norm.*

Below, we restrict the search of optimal controls η_j in (1.4) and ν_i in (1.6) to functions of the form

$$\begin{aligned}
&\eta_j(t) = \textstyle\sum_{\ell=1}^{m} \eta_j^\ell \, \chi_{[t_{\ell-1},t_\ell[}(t) \qquad \text{with} \quad t_0 = 0, \qquad t_\ell > t_{\ell-1}, \qquad t_\ell \in \mathbb{I};\\
&\nu_i(a) = \textstyle\sum_{\ell=1}^{m} \nu_i^\ell \, \chi_{[a_{\ell-1},a_\ell[}(a) \qquad \text{with} \quad a_0 = 0, \qquad a_\ell > a_{\ell-1}, \qquad a_\ell \in \mathbb{R}^+.
\end{aligned}$$

The stability results above ensure that the costs (1.5), (1.7) and (1.8) are Lipschitz continuous functions of the various η_j^ℓ and ν_i^ℓ. Hence, a straightforward Weierstraß argument proves the existence of optimal controls minimizing the costs (1.9) or (1.10).

We refer to [11] for the detailed proofs as well as for further stability estimates on the dependence of the solutions on the various parameters.

3. Qualitative properties

We now compare different instances of both strategies (2.3) and (2.4) by means of numerical integrations.

In all the integrations below, for the convective part we exploit the upwind method [12, § 4.8] with mesh size $\Delta a = 2.5 \cdot 10^{-3}$ along the age axis and $\Delta t = 1.25 \cdot 10^{-3}$ along the time axis. The integrals in the right hand side in (2.1) are computed via a rectangle rule and a fractional step method [12, § 17.1] allows to combine the convective evolution with the source term. The time axis $a = 0$ belongs both to the physical boundary and to the numerical one, its treatment being straightforward since all characteristics move inward the domain $\mathbb{I} \times \mathbb{R}^+$, so that the value of the boundary data can be assigned to the solution. On the other side, along the numerical boundary $a = 10$, the usual free flow conditions is consistent with all characteristic speeds being positive.

Our aim in the integrations below is to clearly show the qualitative properties of the model (2.1). Indeed, we do not claim that the chosen numerical values are realistic. In particular, the most adequate units for t and a might well be different.

With reference to the Cauchy problem (2.1)–(2.2) and to the costs (1.9)–(1.10), we use throughout the following parameters and functions:

$$\begin{aligned}
&d_s(t,a) = \tfrac{1}{4}\,\tfrac{a}{1+a}\,, \qquad d_I(t,a) = \tfrac{1}{2}\,\tfrac{a}{1+a}\,, \qquad d_R(t,a) = \tfrac{1}{4}\,\tfrac{a}{1+a}\,,\\
&r_I(t,a) = \tfrac{1}{10}\,, \qquad \lambda(a,a') = 2\,e^{-|a-a'|/2}\,, \qquad \varphi(a) = 1.
\end{aligned} \tag{3.1}$$

The mortality rates are increasing with age and higher for the infected population. The choice of λ assumes that the infection propagates preferably among individuals of similar age.

We consider two different initial data, first the case without infection, i.e.,

$$S_o(a) = 3\left(1 - \frac{a}{10}\right), \qquad I_o(a) = 0\,, \qquad R_o(a) = \left(1 - \frac{a}{10}\right), \tag{3.2}$$

and then a case with a 20% of infected individuals, with respect to the S population, at time $t = 0$, that is

$$S_o(a) = 2.5\left(1 - \frac{a}{10}\right), \qquad I_o(a) = 0.5\left(1 - \frac{a}{10}\right), \qquad R_o(a) = \left(1 - \frac{a}{10}\right). \tag{3.3}$$

Both these initial data are linearly decreasing with age. Note that the total initial population is the same in the two cases (3.2) and (3.3).

Natality is chosen so that no jump appears between the initial values at $a = 0+$ in (3.2) and the boundary data at $t = 0+$:

$$S_b(t) = 3\,, \qquad I_b(t) = 0\,, \qquad R_b(t) = 1\,, \tag{3.4}$$

where we assume that no individuals are infected already at birth.

3.1. Reference situations

We first consider two extreme situations to be later used for comparisons, namely corresponding to no illness (3.2), and to a spreading illness with no vaccination strategy whatsoever.

In other words, we integrate (2.1)–(2.2)–(3.1) first setting $I_o \equiv 0$, so that for all times t, $I(t) \equiv 0$ and no illness ever appears, and then setting I_o as in (3.3) but dose no vaccination, so that the epidemic spreads uncontrolled. The results of these two integrations are displayed in Figure 1. The two solutions are, clearly, entirely different. When $I \equiv 0$, a sort of dynamic equilibrium is reached, the resulting contour plot being approximately invariant with respect to translation along the vertical t axis. The presence of the I population in the initial datum leads to the spread of the disease and eventually to a dramatic population decrease.

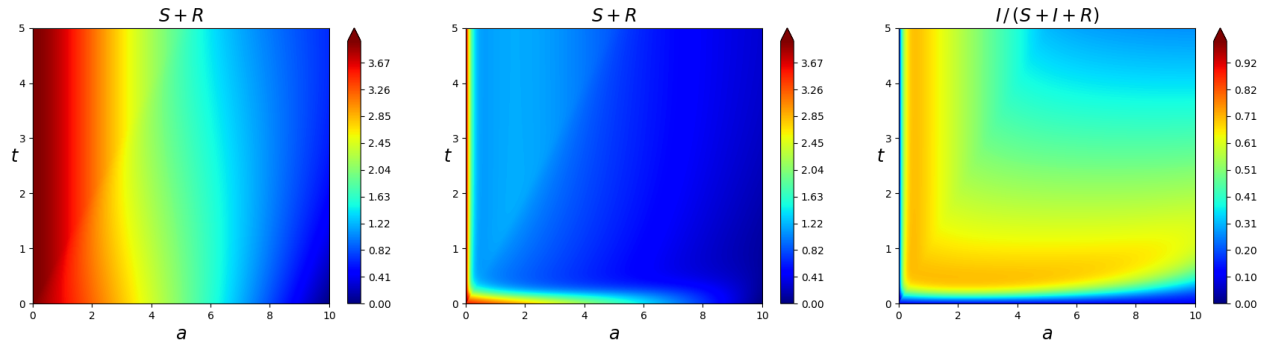

Figure 1. Integration of (2.1), with parameters (3.1), boundary data (3.4), initial data on the left corresponding to (3.2) and, middle and right, to (3.3). The left and middle plots display the sum $S + R$ as a function of t and a, while the rightmost diagram displays the ratio $I/(S + I + R)$ as a function of t and a.

3.2. Vaccinating at specific ages – strategy (2.3)

We consider now a simple vaccination strategy consisting in a single campaign, dosing vaccination at a single age $\bar{a}$ for all times.

As it is to be expected, the earlier vaccinations are dosed, the better it is in terms of the cost (1.8). In Figure 2 the ratio of the number of infected individuals vs. the total population corresponding to the vaccinations ages $\bar{a} = 0.1,\ 0.3,\ 0.5,\ 1.5$ are portrayed. The leftmost contour plot shows the effects of a very early vaccination, clearly far more effective than later doses.

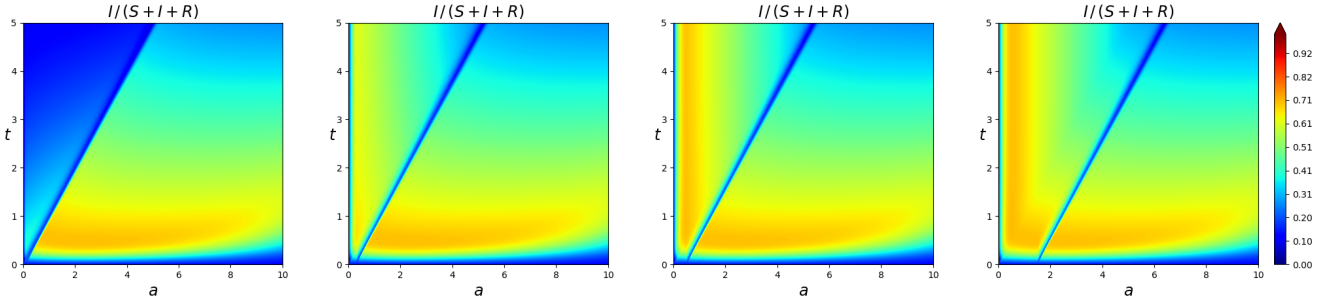

Figure 2. Ratio of the infected population over the whole population in the integration of (2.1), with parameters (3.1), boundary data (3.4) and initial data as in (3.3). The different integrations result from different choices of the age $\bar{a}$ at which *all* S individuals are vaccinated: from left to right: $\bar{a} = 0.1,\ 0.3,\ 0.5,\ 1.5$.

The striking effect of this early age vaccination is confirmed in Figure 3, where we display the sum $S + R$ as a function of t and a in the same cases of the vaccinations ages $\bar{a} = 0.1,\ 0.3,\ 0.5,\ 1.5$. Clearly, due to the form of the vaccination condition (2.3) and to the present smooth data (3.3)–(3.4), the sum $S + R$ is continuous across $\bar{a}$. In the leftmost diagram, the healthy population apparently recovers from the spread of the disease. When vaccinations are dosed at a later age, i.e., in the three diagrams on the right, the relatively large portion of individuals initially vaccinated survive the disease, but juveniles get infected resulting in the solitary waves, consisting essentially of the R population, shown in Figure 3.

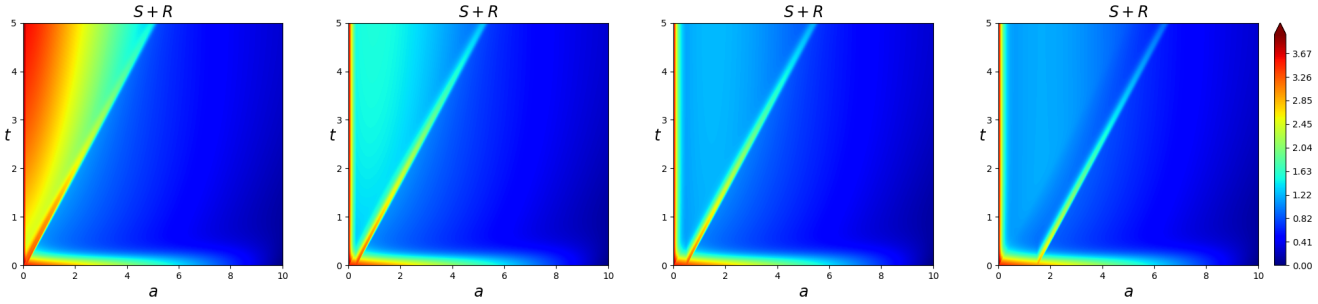

Figure 3. Healthy, i.e., $S + R$, population resulting from the integration of (2.1), with parameters (3.1), boundary data (3.4) and initial data as in (3.3). The different integrations result from different choices of the age $\bar{a}$, at which *all* S individuals are vaccinated, where, from left to right: $\bar{a} = 0.1,\ 0.3,\ 0.5,\ 1.5$.

The counterpart of these solitary waves is the propagating *"hole"* in Figure 2.

In other words, the vaccination campaign at the age $\bar{a} = 0.5$ looks as (un)successful as the campaign at $\bar{a} = 1.5$. On the contrary, dosing at $\bar{a} = 0.1$ is by far more effective.

Indeed, this strategy keeps the density of the susceptible population in (2.1) very low due to (2.3). Hence, also the nonlocal source term, which is proportional to S, is relatively small and infection hardly spreads. When vaccination is dosed at higher ages, the nonlocal source term is able to bring infection at low ages, thus making the vaccination policy far less effective.

Table 1 confirms that, in particular for what concerns the total number of infected individuals, by

far, the best strategy is the one dosing vaccines at the earliest considered age $\bar{a} = 0.1$. This choice also results in the highest number of vaccinated individuals, so that also $\mathcal{N}$ corresponds to the most expensive policy.

Table 1. Value of the functionals in (1.5), (1.8), and (1.9) corresponding to the numerical integration of (2.1) with parameters (3.1), initial datum (3.3) and boundary datum (3.4). The rightmost column refers to the case where no vaccination is dosed.

$\bar{a}$ in (2.3)	0.1	0.2	0.3	0.5	1.0	1.5	none
$\mathcal{J}$ in (1.8)	33.48	41.03	44.73	46.85	47.39	47.51	48.30
$\mathcal{N}$ in (1.5)	10.53	5.05	2.30	0.76	0.41	0.36	0.00
$\mathcal{J} + \mathcal{N}$ in (1.9)	44.01	46.08	47.03	47.61	47.80	47.87	48.30

3.3. Vaccinating at specific times – strategy (2.4)

We now simulate another single vaccination campaign, consisting in dosing all individuals of all ages at a given time $\bar{t}$, see Figure 4.

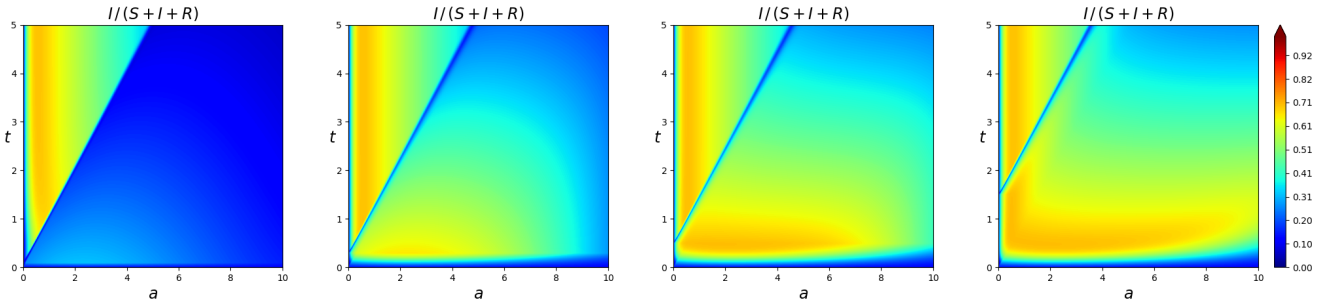

Figure 4. Ratio of the infected population over the whole population in the integration of (2.1), with parameters (3.1), boundary data (3.4) and initial data as in (3.3). The different integrations result from different choices of the time $\bar{t}$, at which *all* S individuals are vaccinated where from left to right, $\bar{t} = 0.1,\ 0.3,\ 0.5,\ 1.5$.

Similarly to the integration detailed in § 3.2, campaigns at earlier times results in being more effective. The choices $\bar{t} = 0.5$ and $\bar{t} = 1.5$ are quite similar to each other and, in the lower right part of the (a, t)–plane, to the situation with no vaccination campaign whatsoever, as it stems from a comparison between the two rightmost diagram in Figure 4 and the rightmost one in Figure 1, see also Table 2.

Note that the present strategy is far less effective: vaccinations are dosed only at the given time $\bar{t}$, after which the disease spreads completely out of control, see Figure 5.

The values of the costs (1.7), (1.8) and (1.10) presented in Table 2 show that vaccinating the whole S population at $\bar{t} = 0.5$ or later, makes relatively small difference, the most convenient choice being at the earliest time $\bar{t} = 0.1$. Similarly to what happens in § 3.2, vaccinating all susceptible individuals at $\bar{t} = 0.1$ makes the susceptible portion of the population very small wherever $a > t - \bar{t}$, thus essentially canceling the nonlocal source term which represents the spreading of the disease.

We note however an evident key difference between the best vaccination age choice (i.e., $\bar{a} = 0.1$) in § 3.2 and the present best vaccination time choice (i.e., $\bar{t} = 0.1$). The latter one yields lower values of the chosen costs. However, as time grows, the former strategy is prone to by far preferable evolutions. Indeed, the leftmost diagram in Figure 2 (corresponding to $\bar{a} = 0.1$) clearly shows a *decreasing* I population, while it is *increasing* in the latter strategy, see Figure 4, left (corresponding to $\bar{t} = 0.1$).

Table 2. Value of the functionals in (1.7), (1.8) and (1.10) corresponding to the numerical integration of (2.1) with parameters (3.1), initial datum (3.3) and boundary datum (3.4). The rightmost column refers to the case where no vaccination is dosed.

$\bar{t}$ in (2.4)	0.1	0.2	0.3	0.5	1.0	1.5	none
$\mathcal{J}$ in (1.8)	31.71	38.80	43.65	46.79	47.40	47.42	48.30
$\mathcal{N}$ in (1.7)	9.37	5.46	2.74	0.86	0.40	0.39	0.00
$\mathcal{J} + \mathcal{N}$ in (1.10)	41.08	44.26	46.39	47.66	47.80	47.80	48.30

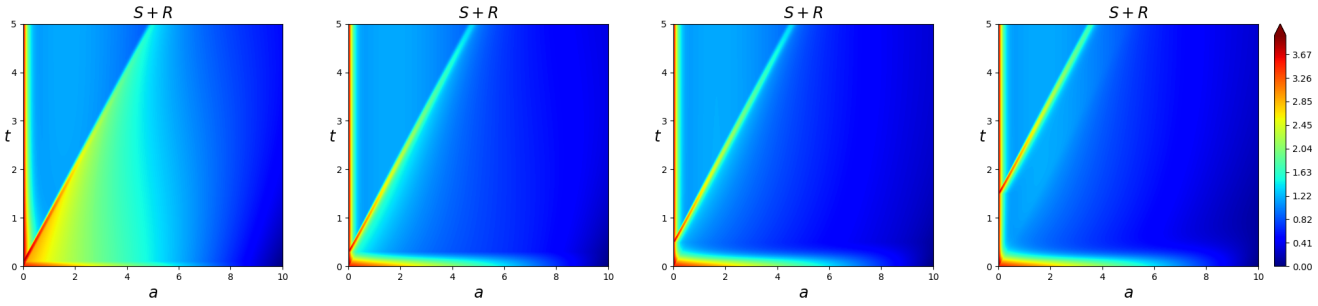

Figure 5. Healthy, i.e., $S + R$, population resulting from the integration of (2.1), with parameters (3.1), boundary data (3.4) and initial data as in (3.3). The different integrations result from different choices of the time $\bar{t}$, at which *all* S individuals are vaccinated where from left to right, $\bar{t} = 0.1,\ 0.3,\ 0.5,\ 1.5$.

4. Optimizing a vaccination strategy

We now consider in more detail the search for an optimal vaccination strategy in a slightly different setting. First, we assume that infection among individuals of different ages is somewhat more difficult, slightly modifying (3.1) to

$$\begin{array}{lll} d_s(t,a) = \frac{1}{4}\,\frac{a}{1+a}\,, & d_I(t,a) = \frac{1}{2}\,\frac{a}{1+a}\,, & d_R(t,a) = \frac{1}{4}\,\frac{a}{1+a}\,, \\ r_I(t,a) = \frac{1}{10}\,, & \lambda(a,a') = e^{-2|a-a'|}\,, & \varphi(t) = 1\,, \end{array} \tag{4.1}$$

and choose the initial datum

$$\begin{aligned} S_o(a) &= \begin{cases} 3.0\left(1-\frac{a}{10}\right) & a \in [0,3] \cup [5,10] \\ 1.5\left(1-\frac{a}{10}\right) & a \in]3,5[\end{cases} \\ I_o(a) &= \begin{cases} 0 & a \in [0,3] \cup [5,10] \\ 1.5\left(1-\frac{a}{10}\right) & a \in]3,5[\end{cases} \\ R_o(a) &= \left(1-\frac{a}{10}\right). \end{aligned} \tag{4.2}$$

corresponding to an initial infected population that amounts to 50% of the susceptible population in the age interval $]3, 5[$. As boundary data, we keep the choice (3.4), corresponding to a constant natality rate for the S and R populations, and to no one being infected at birth.

As a first reference situation, we consider the case of no vaccination being dosed to anyone. The resulting integration is displayed in Figure 6.

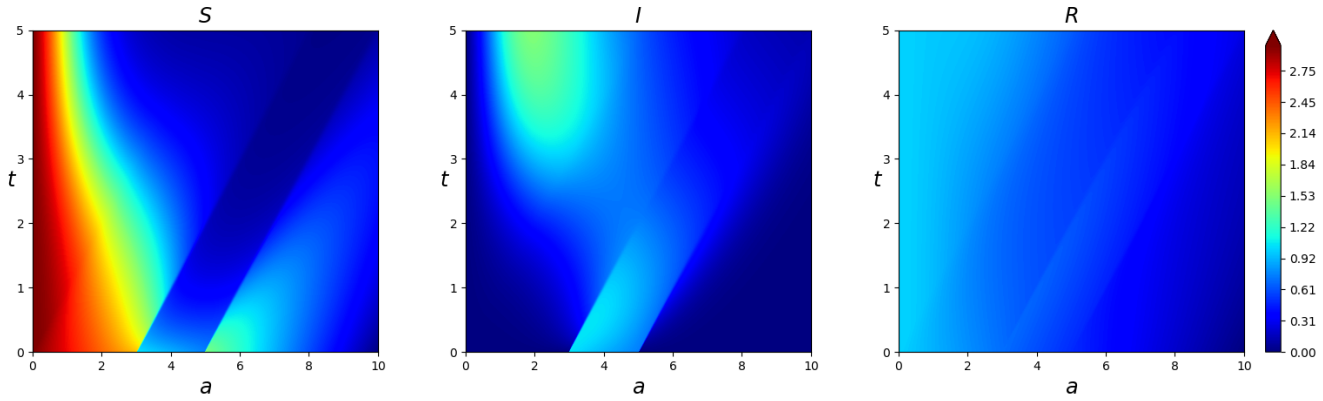

Figure 6. Integration of (2.1)–(2.2) with parameters (4.1), initial datum (4.2) and boundary inflow (3.4). From left to right: the S, I and R plots. Note the rise in the I population in the region $t \geq 3$ and $a \in [1, 3]$, a clear effect of the nonlocal source terms in (2.1) modeling the spread of the infection.

In this reference case, the total number of infected individuals is 22.77.

We only remark that Figure 6 shows a typical effect of the nonlocality of the source terms in (2.1). There is an increase in the I population for, approximately, $t \geq 3$ and $a \in [1, 3]$ due to the transmission and growth of the infection, a feature which becomes relevant in regions close to (relatively) high values of the susceptible population S.

Below we restrict the values of the percentages η_j and ν_i in (2.3) and (2.4) to the interval $[0, 0.8]$. Indeed, it is reasonable to assume that not *every* individual can be vaccinated and that, in some cases, vaccination may fail to immunize a small percentage of susceptible individuals. For the sake of simplicity, we introduce only three vaccination ages $\bar{a}_1$, $\bar{a}_2$ and $\bar{a}_3$ or times $\bar{t}_1$, $\bar{t}_2$ and $\bar{t}_3$.

We present both sample values of the costs (1.9)–(1.10) and the results of optimization procedures. The former correspond to dosing vaccines to 60% or 80% of the S population at each prescribed age for all times, or at each prescribed time at all ages. The latter are achieved through the usual *descent method*, see [13, § 7.2.2], with suitable projections that restrict to values of η_1, η_2, η_3 and ν_1, ν_2, ν_3 in $[0, 0.8]$. A formal justification of the use of this method is in the Lipschitz continuous dependence of the cost (1.9) or (1.10) on the various parameters, see [11].

In the integrations below, we keep $\Delta a = 2.5 \cdot 10^{-3}$ and $\Delta t = 1.25 \cdot 10^{-3}$. However, due to computing time limitations, when applying the steepest descent method we passed to coarse meshes, where $\Delta a = 5 \cdot 10^{-2}$ and $\Delta t = 2.5 \cdot 10^{-2}$. Correspondingly, in case of the controls (2.3), optimal controls are sought in the class of locally constant functions of the type $\eta_j(t) = \sum_{\ell=1}^{20} \eta_j^\ell \chi_{[(\ell-1)/4,\, \ell/4[}(t)$. An entirely similar procedure is followed in the case of the age dependent controls (2.4). For completeness, we recall that in the present merely Lipschitz continuous setting, the steepest descent (or gradient) method needs not

converge and, even if it does, its limit may well be different from a point of minimum. Therefore, in our application of this method, we keep checking that the values of the cost (do indeed) decrease, but we can not ensure that the values obtained are indeed points of minimum.

4.1. Dosing vaccinations at prescribed ages

Now, in the model (2.1)–(2.2) with parameters (4.1), initial datum (4.2) and boundary datum (3.4) we prescribe 3 vaccination ages and, correspondingly, 3 constant values of the percentage of vaccinated individuals, so that, with reference to the notation (2.3),

$$\bar{a}_1 = 2.0\,, \qquad \bar{a}_2 = 4.0\,, \qquad \bar{a}_3 = 6.0 \quad \text{and} \quad \eta_j \in \{0.6\,,\ 0.8\} \text{ for } j = 1, 2, 3\,. \tag{4.3}$$

First, we perform the resulting 8 numerical integrations and record the resulting costs (1.5), (1.8) and (1.9). Then, these costs are compared among each other and with the costs resulting from the steepest descent method. The numerical values obtained are in Table 3.

Table 3. Costs resulting from the integrations of model (2.1)–(2.2) with parameters (4.1), initial datum (4.2), boundary datum (3.4) and control (2.3) with parameters (4.3).

η_1	η_2	η_3	$\mathcal{J}$ as in (1.8)	$\mathcal{N}$ as in (1.5)	$\mathcal{J} + \mathcal{N}$ as in (1.9)
0.6	0.6	0.6	14.54	7.56	22.11
0.6	0.6	0.8	14.38	7.87	22.25
0.6	0.8	0.6	14.18	8.02	22.20
0.6	0.8	0.8	14.02	8.31	22.83
0.8	0.6	0.6	13.12	9.22	22.34
0.8	0.6	0.8	12.96	9.52	22.48
0.8	0.8	0.6	12.80	9.60	22.40
0.8	0.8	0.8	12.64	9.88	22.53
see Figure 8			16.01	4.67	20.69

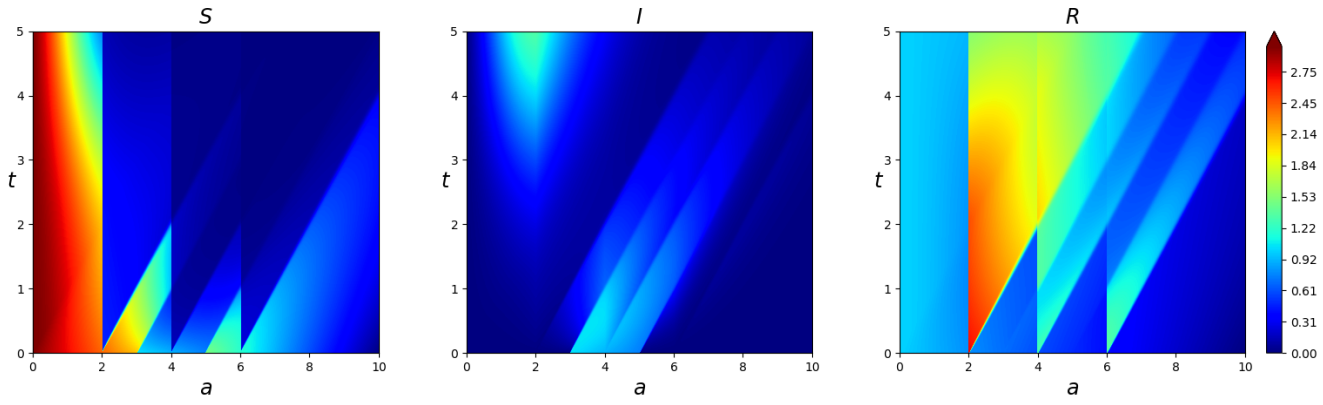

Figure 7. Contour plots of the solution to model (2.1)–(2.2) with parameters (4.1), initial datum (4.2), boundary datum (3.4) and control (2.3) with $\bar{a}_1 = 2.0$, $\bar{a}_2 = 4.0$, $\bar{a}_3 = 6.0$ and $\eta_1 = \eta_2 = \eta_3 = 0.8$.

As is to be expected, the lowest amount of infected individuals results from the highest (and most expensive) vaccination dosing, detailed in Figure 7. There, the discontinuities in S across the ages $\bar{a}_j$ resulting from the conditions (2.3) are clearly visible. Choosing $\bar{a}_1 = 2.0$ as the lowest vaccination age allows, for about $t \geq 4$, that individuals younger that this age are infected and, at later times, the disease may well spread among juveniles.

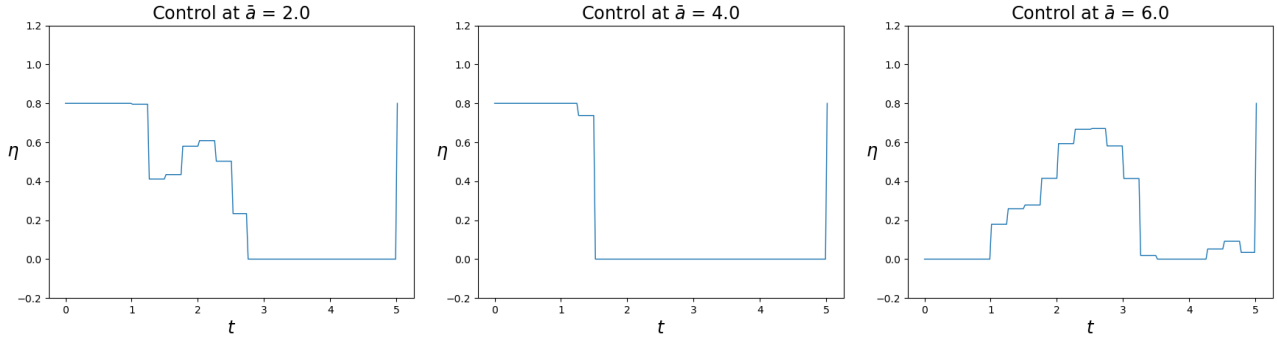

Figure 8. Optimal time dependent controls found by means of the descent method applied to minimize the cost (1.9), corresponding to the integration in Figure 9.

The steepest descent procedure yields a value of the cost $\mathcal{J} + \mathcal{N}$ in (1.9) lower than any of the ones obtained with constant η_j as in (4.3), see Table 3. The optimal controls found by means of the steepest descent method are shown in Figure 8 and the corresponding solutions are in Figure 9.

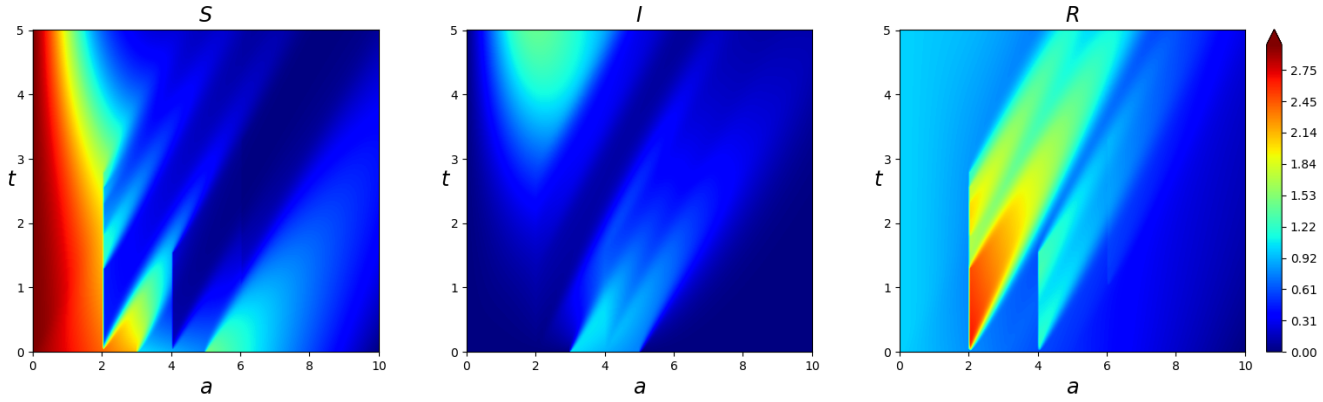

Figure 9. Contour plots of the solutions to to model (2.1)–(2.2) with parameters (4.1), initial datum (4.2), boundary datum (3.4), optimized with respect to the controls η_1, η_2, η_3 in (2.3).

4.2. Dosing vaccinations at prescribed times

We now follow a procedure, in a sense, analogous to that detailed in the preceding Paragraph 4.1. Choose the times and controls

$$\bar{t}_1 = 0.5\,, \qquad \bar{t}_2 = 1.0\,, \qquad \bar{t}_3 = 1.5 \qquad \text{and} \qquad \nu_i \in \{0.6\,, 0.8\} \text{ for } i = 1, 2, 3\,. \tag{4.4}$$

The costs of the integrations resulting from these choices and from the optimization are collected in Table 4. Again, the lowest number of infected individuals is obtained with the highest number of vaccinations and the corresponding solutions are plotted in Figure 10.

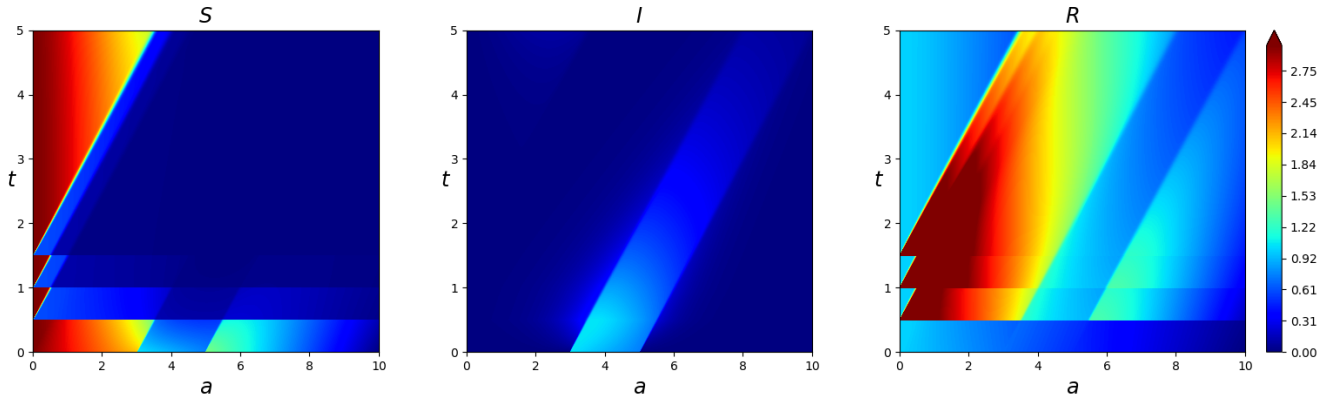

Figure 10. Contour plots of the solution to model (2.1)–(2.2) with parameters (4.1), initial datum (4.2), boundary datum (3.4) and control (2.4) with $\bar{t}_1 = 0.5$, $\bar{t}_2 = 1.0$, $\bar{t}_3 = 1.5$ and $\nu_1 = \nu_2 = \nu_3 = 0.8$.

Given that infected individuals can not turn back susceptible, it is clear that the first vaccination of 80% of all susceptible individuals greatly hinders the spreading of the disease. The later vaccinations, dosed also to the newly born individuals, block further infections, see Figure 10.

Table 4. Costs resulting from the integrations of model (2.1)–(2.2) with parameters (4.1), initial datum (4.2), boundary datum (3.4) and control (2.4) with parameters (4.4).

ν_1	ν_2	ν_3	$\mathcal{J}$ as in (1.8)	$\mathcal{N}$ as in (1.7)	$\mathcal{J} + \mathcal{N}$ as in (1.10)
0.6	0.6	0.6	6.41	13.05	19.47
0.6	0.6	0.8	6.23	13.75	19.98
0.6	0.8	0.6	6.17	13.60	19.77
0.6	0.8	0.8	6.06	14.10	20.16
0.8	0.6	0.6	5.78	13.89	19.66
0.8	0.6	0.8	5.67	14.44	20.12
0.8	0.8	0.6	5.66	14.22	19.88
0.8	0.8	0.8	5.59	14.65	20.24
see Figure 11			7.80	8.18	15.98

The strategy found through the steepest descent method, shown in Figure 11, clearly takes advantage of the particular shape of the initial datum (4.2). Indeed, the two *"humps"* in ν_2 and ν_3 roughly correspond to the wave of infected individuals propagating from $t = 0$ onward.

As a consequence, note that the optimal control ν_3 vanishes for small ages. This is due to the fact that newborn are healthy and that the preceding vaccination campaigns succeeded in avoiding the transmission of the infection to the youngest part of the population, see Figure 12.

With the data chosen in (4.1) and the parameters (4.2), the best vaccination strategies turn out to be the ones of the type (2.4), i.e., those where a percentage $\nu_i(a)$ of all susceptible individuals of age a are dosed at time $\bar{t}_i$, as it stems out comparing Table 3 with Table 4. Clearly, this outcome is a consequence of the particular choices in (4.1) and (4.2), but the framework based on (2.1) and (2.3) or (2.4), and its amenability to optimization procedure, is independent of these choices.

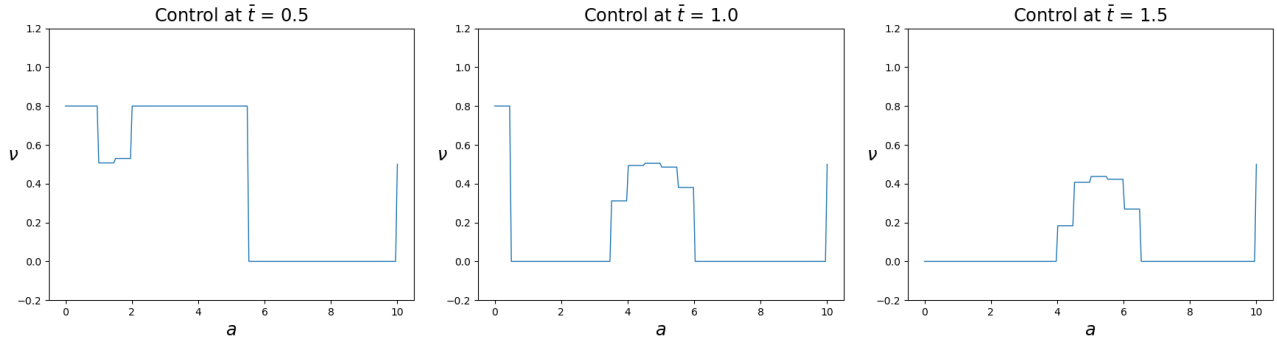

Figure 11. Plots of the optimal age dependent controls ν_1, ν_2, ν_3 found by means of the descent method applied to minimize the cost (1.10).

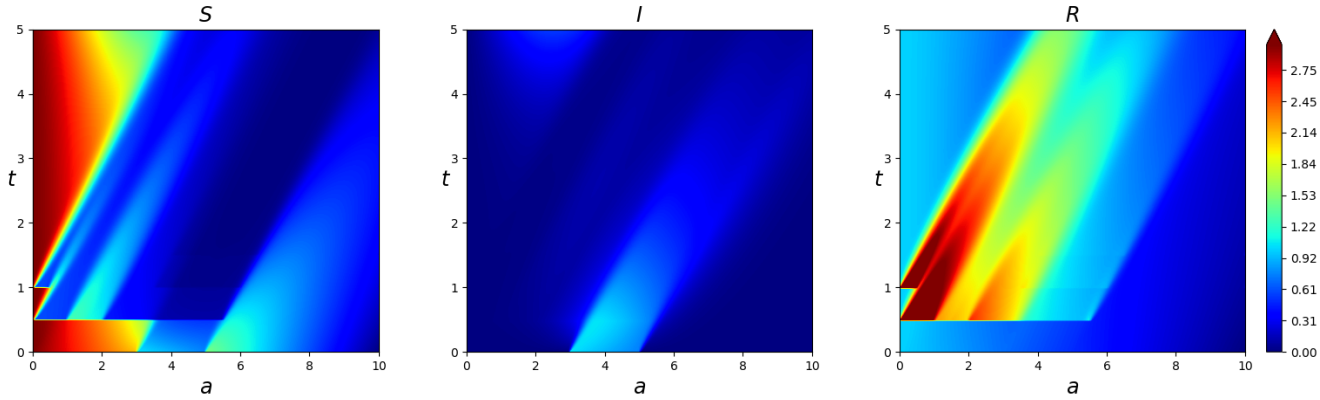

Figure 12. Contour plots of the solutions to model (2.1)–(2.2) with parameters (4.1), initial datum (4.2), boundary datum (3.4), optimized with respect to the controls ν_1, ν_2, ν_3 in (2.4).

5. Conclusions

We addressed the issue of optimizing vaccination strategies. Sample numerical integrations show various features of the solutions to the integro–differential model (2.1)–(2.2) and the effects of different choice of the controls η_j in (2.3) or ν_i in (2.4). Standard numerical optimization procedures, such as the steepest descent method, can be applied to single out optimal choices of the controls.

The present framework is amenable to a variety of different applications and extensions, only a minor part of which were explicitly considered above. For instance, natality, which is represented by the boundary datum, can be assigned as a function of the present, or past, population densities, also allowing for newborn to be infected also at birth. The present age structured formulation allows to take into account the possibility that the disease is transmitted differently in different age groups. Introducing in the S, I or R populations sexual distinctions only amounts to consider more equations, the basic analytic framework in [11] remaining essentially unaltered.

Acknowledgments

Part of this work was supported by the PRIN 2015 project *Hyperbolic Systems of Conservation Laws and Fluid Dynamics: Analysis and Applications* and by the GNAMPA 2018 project *Conservation Laws: Hyperbolic Games, Vehicular Traffic and Fluid dynamics*.

The *IBM Power Systems Academic Initiative* substantially contributed to the numerical integrations.

Conflict of interest

The authors declare there is no conflict of interest.

References

1. W. O. Kermack, A. G. McKendrick, G. T. Walker, A contribution to the mathematical theory of epidemics, *Proc. R. Soc. London. Ser. A, Containing Papers of a Mathematical and Physical Character*, **115** (1927), 700–721.
2. H. Inaba, Age-structured sir epidemic model, in *Age-Structured Population Dynamics in Demography and Epidemiology*, Springer Singapore, Singapore, 2017, 287–331.
3. J. D. Murray, *Mathematical biology. I*, vol. 17 of Interdisciplinary Applied Mathematics, 3rd edition, Springer-Verlag, New York, 2002, An introduction.
4. B. Perthame, *Transport equations in biology*, Frontiers in Mathematics, Birkhäuser Verlag, Basel, 2007.
5. H. Behncke, Optimal control of deterministic epidemics, *Optim. Contr. Appl. Met.*, **21** (2000), 269–285.
6. H. Gaff, E. Schaefer, Optimal control applied to vaccination and treatment strategies for various epidemiological models, *Math. Biosci. Eng.*, **6** (2009), 469–492.
7. H. R. Joshi, S. Lenhart, M. Y. Li, L. Wang, Optimal control methods applied to disease models, in *Mathematical studies on human disease dynamics*, vol. 410 of Contemp. Math., Amer. Math. Soc., Providence, RI, 2006, 187–207.
8. A. El-Alami Laaroussi, M. Rachik, M. Elhia, An optimal control problem for a spatiotemporal SIR model, *Int. J. Dyn. Control*, **6** (2018), 384–397.
9. L.-M. Cai, C. Modnak, J. Wang, An age-structured model for cholera control with vaccination, *Appl. Math. Comput.*, **299** (2017), 127–140.
10. G. B. Folland, *Real analysis*, Pure and Applied Mathematics (New York), John Wiley & Sons Inc., New York, 1984, Modern techniques and their applications, A Wiley-Interscience Publication.
11. R. M. Colombo, M. Garavello, Well posedness and control in a nonlocal sir model, 2019. Available from: `http://arxiv.org/abs/1910.07389`, Preprint, arXiv 1910.07389.
12. R. J. LeVeque, *Finite volume methods for hyperbolic problems*, Cambridge Texts in Applied Mathematics, Cambridge University Press, Cambridge, 2002.

13. A. Quarteroni, R. Sacco, F. Saleri, *Numerical mathematics*, vol. 37 of Texts in Applied Mathematics, Springer-Verlag, New York, 2000.